NRL REPORT 3687

FR 3687

ANALYSIS OF THE AUTOMATIC CARRIER CONTROLLED APPROACH SYSTEM

NAVAL RESEARCH LABORATORY

WASHINGTON, D.C.

NRL REPORT 3687

ANALYSIS OF THE AUTOMATIC CARRIER CONTROLLED APPROACH SYSTEM

Joseph B. Reynolds, Jr. and Irving M. Saffitz

May 25, 1950

Approved by:

Mr. Albert Brodzinsky, Head, Avigation Branch
Dr. R. M. Page, Superintendent, Radio Division III

NAVAL RESEARCH LABORATORY

CAPTAIN F. R. FURTH, USN, DIRECTOR

WASHINGTON, D.C.

DISTRIBUTION

CNO	5
ONR	
Attn: Code 461	3
Attn: Code 467	1
Attn: Code 470	1
Attn: Code 489	1
BuShips	
Attn: Code 915	2
BuAer	
Attn: Code EL-3	2
Attn: Code EL-4	1
Attn: Code MR-5	1
Attn: Code TD-4	2
ComOpDevFor	2
Dir., SDC, Sands Point	3
CDR, NATC	3
Supt., USNPGS	1
CO, USNATTC, Memphis	1
CO, FAWTULANT	1
CO, FAWTUPAC	1
Dir., USNEL	2
CDR, USNOTS	
Attn: Reports Unit	2
SNLO, USNELO	1
CO, NADS	2
OCSigO	
Attn: Ch. Eng. & Tech. Div., SIGTM-S	1
CO, SCEL	
Attn: Dir. of Eng.	2
Wright-Patterson AFB	
Attn: CADO	2
Attn: Ch., Electronics Subdiv., MCREEO-2	1
CO, Watson Labs., AMC, Red Bank	
Attn: ENR	1
CO, Air Force Cambridge Field Station	
Attn: ERRS	1
ANDB	
Attn: Navy Member	3
Dir., NBS	
Attn: CRPL	1
RDB	
Attn: Information Requirements Branch	2
Attn: Navy Secretary	1
Naval Res. Sec., Science Div., Library of Congress	
Attn: Mr. J. H. Heald	2

CONTENTS

ABSTRACT

This report covers an analysis of the operational and technical requirements of an Automatic Carrier Controlled Approach (ACCA) system for carrier aircraft all-weather operation. There is a discussion of a detailed system proposal for aircraft turn axis control and of the functional requirements imposed on the system components. Turn axis dynamics have been studied both in the time and frequency domains, and the results obtained justify the application of standard servo engineering procedures to the control problem. By employing Fourier analysis, the frequency compositions of data and control variables have been obtained, and the frequency bandwidth requirements imposed on the system are examined. Two specific proposals for altitude control are outlined in terms of two different techniques employed in aircraft height position determination. A detailed discussion brings out the relationship of carrier deck motions to aircraft position data and to aircraft control. The future research program on ACCA is outlined.

PROBLEM STATUS

This is an interim report on the problem; work is continuing.

AUTHORIZATION

NRL Problem R04-42R, CNO Aviation Plan No. 73
NR 504-420

TABLE OF SYMBOLS

x	Perpendicular distance of the aircraft from the derived path
$\dot{x}$	Time rate of change of perpendicular distance
E_h	Error signal controlling altitude of the aircraft
E_s	Error signal controlling the lateral position of the aircraft
h_c	Computed altitude
h_m	Measured altitude
k_1	Lateral error control proportionality constant
k_2	Lateral error lead proportionality constant
w_{01}	Gain constant of the aircraft and autopilot in the yaw axis
w_{02}	Gain constant of the aircraft and autopilot in the pitch axis
R_a	Actual slant range
R_m	Measured slant range
$s(t)$	Variable speed of aircraft along the flight path
α	Heading error of aircraft measured with respect to the flight path tangent
$\dot{\alpha}$	Time rate of change of heading error
γ	Angle of attack of aircraft
$\dot{\gamma}$	Time rate of change of angle of attack
θ_a	Actual azimuth of aircraft with respect to the line parallel to the fore-aft line of the carrier and passing through the radar site
θ_m	Measured azimuth of aircraft with respect to the line parallel to the carrier fore-aft line and passing through the radar site
θ_c	Desired azimuth of the aircraft with respect to the line parallel to the fore-aft line of the carrier and passing through the radar site
β	Absolute heading of aircraft measured with respect to the line parallel to the fore-aft line of the carrier and passing through the radar site
$\dot{\beta}$	Time rate of change of absolute heading
$\Delta\theta$	Azimuth error of aircraft where $\Delta\theta = \theta_c - \theta_m$
β_r	The angle that the tangent to the path makes with the line parallel to the fore-aft line of the carrier and passing through the radar site

$gh(p)$	Open loop transfer function of auto-land servo with certain idealized assumptions
$h(p)$	Transfer function for the aircraft cascaded with that of the flight path geometry
$g(p)$	Transfer function of the lead network
Φ_a	Actual elevation angle of the aircraft with respect to the horizontal established for the radar site
$l(p)$	LaPlace transform of the load disturbance
$E_S(p)$	LaPlace transform of the error signal
$v(p)$	LaPlace transform of desired aircraft position
$r(p)$	LaPlace transform of regulated aircraft position
Φ_m	Measured elevation angle of aircraft
ϕ_m	Phase margin of open loop transfer function
G_o	Gain constant of lead network
T_A	Time constant of lead network
$x(p)$	LaPlace transform of the displacement error
$\alpha(p)$	LaPlace transform of the instantaneous heading error
w	Angular frequency in radians/sec
ω	Angular frequency normalized with respect to T_A
w_{co}	Cut off frequency of $x(jw)$
w_c	Frequency beyond which auto-pilot aircraft combination breaks down as a pure integrator

ANALYSIS OF THE AUTOMATIC CARRIER CONTROLLED APPROACH SYSTEM

INTRODUCTION

As a major portion of its work for implementing the ONR assignment in CNO Aviation Plan No. 73, the Naval Research Laboratory has set up a program of research on an automatic carrier controlled approach system hereafter referred to as ACCA, Reference (1). The need for a successful all weather automatic carrier approach system is readily evident, from both tactical and operational considerations. A discussion of some of these tactical and operational considerations is to be found in the appendix covering observations made by NRL personnel of carrier operations during operation PORTREX.

Two successful approach systems for shore-based operation are the GCA and ILS systems. The GCA system uses precision radar determination of aircraft position, and voice talk-down of the aircraft along a predetermined approach path. The ILS system generates an approach path in the air by means of a pair of crossed electro-magnetic beams. The angular deviation of the aircraft from the approach path appears as a visual deflection of a crossed-pointer meter. The pilot then controls the aircraft position to "zero," the crossed-pointer meter. Both systems are undergoing extensive research to provide completely automatic approach with pilot intervention only in the touchdown phase, Reference (2).

The carrier automatic approach problem presents most of the technical and operational difficulties of the automatic GCA and automatic ILS systems. The problem is further complicated by the fact that a carrier landing strip is a generally unstable platform of relatively minute dimensions. Thus, system resolution requirements are necessarily more stringent, and the attendant problem of correlating aircraft control with deck motions becomes a vital link in the system.

This report covers the theoretical work done on the problem from 1 January 1949 until 25 May 1950. The report consists of two major portions. First, a detailed discussion is given of the over-all system proposal and of the various units making up the total system. Second, a theoretical analysis of system performance is given. A detailed study of system dynamics in the time domain was followed by a frequency domain analysis of the system as a closed servo loop. The theoretical system performance was evaluated by this procedure. A subsequent report covering circuitry, instrumentation, and engineering details of the experimental model equipment will follow at an early date.

SYSTEM PROPOSAL

The system proposed for the turn axis control as well as elevation control is in essence a closed servo loop. The position data of the aircraft are derived by means of a

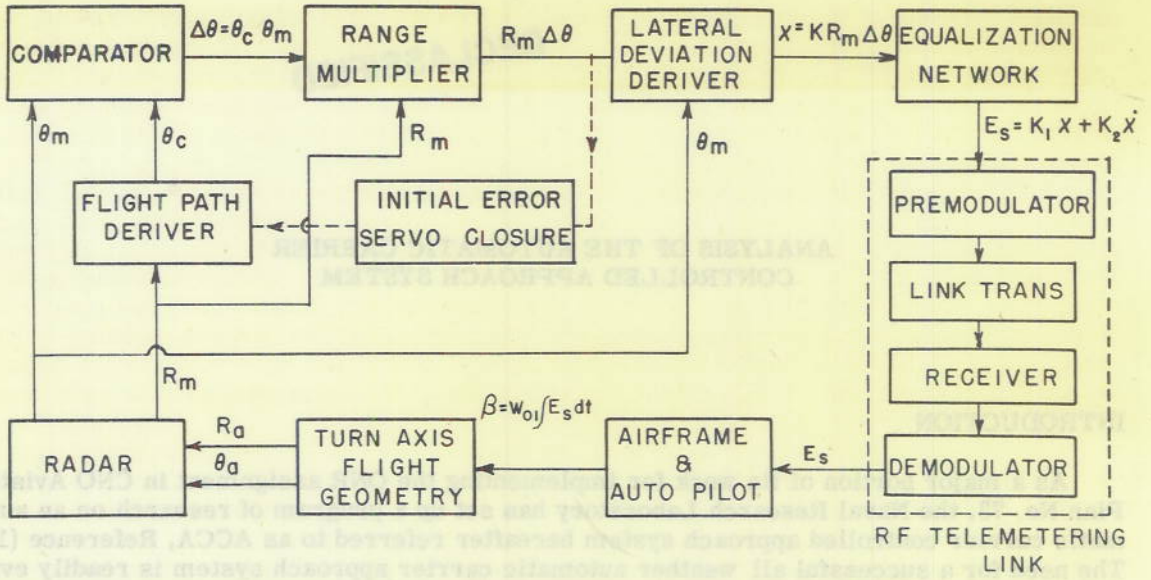

Figure 1 - Proposed ACCA system block diagram for turn axis control

radar sited on the carrier. By comparing these data with the desired position data, suitable error signals are derived. These error signals are telemetered to the aircraft under control by means of a radio link and are applied to the automatic pilot (autopilot) and aircraft combination to close out the error. The heading change of the aircraft due to the error signals results in a new position of the aircraft thereby closing the loop, the new position data being again determined by the radar. Thus the control line represents a closed servo loop. A functional block diagram of the proposed system is shown on Figure 1.

FUNCTIONAL DISCUSSION OF BLOCK DIAGRAM

Radar

The position data gathering function in the ACCA system may be performed by a radar. The radar must be capable of tracking the target aircraft from maximum range at capture of approximately 8000 yards to the minimum range at final approach of approximately 150 yards. Range accuracies in the order of ± 10 yards and angular tracking accuracies of better than ± 2^0 (or lateral displacement about touchdown path center line of ± 5 yards) are necessary. Further, the radar must be able to track low flying aircraft without ambiguity which requires low angle tracking in the presence of maximum "sea returns." This implies the need for MTI or doppler radars to obtain stable, reliable data gathering in the region of minimum range.

The carrier flight deck and hence radar site is a generally unstable platform moving relative to a fixed co-ordinate system in the roll, pitch, and yaw axes, and also in heave. The effect of these carrier deck motions on the control problem must be analyzed in terms of the data gathering properties of the radar as well as the requirements on system response time.

Carrier deck motions have negligible effect on the radar determination of slant range. Further, since the radar site moves in synchronism with the carrier deck, elevation data

derived from the radar require no correction for heave. The altitude flight course, however, is generated with respect to the carrier deck; and as the deck moves in heave, the flight course will move in synchronism with the deck. Thus, an aircraft which was on course prior to carrier heave is now off course. Carrier heave then may be analyzed as a desired state disturbance on the altitude control loop.

If aircraft altitude is determined from unstabilized radar elevation data, then roll and pitch of the carrier deck will effect determination of aircraft altitude. When the aircraft is abeam of the carrier, measured elevation will be in error by the amount of carrier roll. When the aircraft is dead aft of the carrier, measured elevation will be in error by the amount of carrier pitch. At intermediate positions, the elevation error will be some combination of carrier roll and pitch. Thus, elevation data must be corrected either by gyrostabilizing the radar mount in roll and pitch, or by subtracting deck motion data (obtained by means of a roll and pitch stabilized platform) from the unstabilized radar data.

The effect of carrier yaw is a more complicated one. Since the control flight course is generated with respect to the carrier center line, as the carrier deck moves in yaw the flight course moves with it. It should be emphasized that no correction of radar data is desired, since aircraft azimuth must be measured with respect to the carrier center line. However, an aircraft which was on course prior to carrier yaw is now off course. Thus, carrier yaw may be analyzed in the form of a desired state disturbance. The configuration of the present flight path (to be described later) is such that the maximum lateral deviation of the aircraft from the flight path due to yaw occurs at a range of 4,750 yards and the magnitude of the deviation is 75 yards for 1^{0} yaw. Anticipated carrier yaw periods are in excess of 10 sec, thus it is expected that the control loop will experience no difficulty in closing out errors resulting from carrier yaw. In the region of critical control, or minimum range, the flight path is very nearly a straight line passing through the carrier center line. Carrier yaw of 1^{0} will result in an error of 1/60 times range or 10 yards at 600 yards range. With stiff control in this region, no difficulty in course following is expected. In general, a more complete analysis of this problem in terms of flight data must be made.

The two types of radar systems which received consideration for the data gathering function are track-while-scanning radars and automatic continuously tracking radars. It should also be pointed out that the system is sufficiently flexible to permit substitution of other radars to perform the data gathering function. Thus, if and when FM doppler radars (which will provide very short range resolution) and MTI becomes available, their incorporation into the system can be readily accomplished.

Both track-while-scanning and automatic continuously tracking radars offer distinct advantages. Tracking-while-scanning radar systems are now under development at the Watson Laboratory of the USAF's Air Materiel Command and at industrial laboratories. The advantage of such a radar is the use of a single antenna system for multiple aircraft in the control phase. A disadvantage of such a system, in addition to a high degree of complexity, is the physical limitations placed on high speed rotation of the relatively large antenna masses required. However, this may be eliminated by electronic scanning as is done in the Automatic Ground Controlled Approach system. Present data indicate scanning speeds in the order of four looks per second can be expected although experimental scanning speeds which are several orders of magnitude greater have been obtained. This means that position data are available at quarter-second intervals, or with 90-knot airspeed aircraft flying dead aft of a 30-knot carrier,* one "look" every 25 feet. On the other hand, a single

---

* Carrier speed is normally regulated so that air mass moves at approximately 30 knots over the deck during landing operations.

continuously tracking radar could provide position data at the pulse repetition frequency, or once in a 1/2000-second, or at 1/20-foot intervals.

A second disadvantage is that all the position data is dependent on the continued operation of one radar and its failure would interrupt all automatic approaches completely.

The latter fault can be avoided by using multiple radars, i.e., one radar per aircraft under control. This is possible with radars similar to the AN/APG series of airborne gunlaying equipments since such equipments are quite small and compact. The AN/APG-3 for example, which NRL is using in the initial portions of its experimental program, weighs less than 300 pounds and has an antenna only 12 inches in diameter. The use of three or four such radars would insure noninterruption of service if breakdown occurs, provided the procedures for target assignments, tracking coordination, etc., can be worked out. Other reasons for using this radar for the experimental program at NRL are (1) that its compactness allows it to be mounted in a single truck with test and recording instruments, thus providing an extremely mobile field unit and (2) that it avoids the necessity for the development and construction of tracking-while-scanning equipments.

After slight modification of the range tracking circuitry, the maximum track range of the AN/APG-3 has been extended beyond 8,000 yards. The specified angular tracking accuracy of the radar is $\pm 1/4^{\circ}$ which is well within the required limits. The range tracking accuracy is ± 12.5 yards which appears to be adequate. The theoretical minimum range of the radar, with 1/2 μsec pulses is 82 yards, assuming infinite bandwidth and zero recovery time for the receiver. The probably usable minimum range of the radar is in the order of 150 yards, which appears to be adequate for the final approach.

An operational problem indigenous to all radar data gathering systems is that of capture of the aircraft to be controlled. Preliminary investigations of the AN/APG-3 radar indicates that some of the inherent difficulties in capture can be resolved by experienced operators. Further evaluation of the capture problem will have to be made and procedures worked out to eliminate undesirable time delays in control due to the time interval required for capture.

Flight Path Deriver

The primary function of the flight path deriver is to generate the desired control path with respect to the carrier that the airplane is to follow. Measured range information from the radar is fed into the deriver, and θ_c, the desired azimuth, becomes the output.

To be tactically acceptable at present, the control path should conform to that used under contact conditions, i.e., roughly a semicircular arc starting abeam of the carrier and ending at the flight deck ramp. It is highly undesirable to use long dead aft approaches due to the necessity for stringing multiple aircraft out behind the carrier, and due to traffic control problems incident to any wave-off. Further, greater isolation of several carriers in a fleet unit would ne necessary to prevent possible radar capture of aircraft belonging to other carrier groups. Discussion of operationally acceptable flight paths is contained in an appendix following this report.

In any case, no path contour can be allowed for which maximum safe rate of turn for low flying aircraft is exceeded, either along the path or during close-out of transients. Consistent with these requirements, it was decided to generate an approximately semicircular path with a diameter of 7,500 yards as shown in Figure 2. The standard contact final turn is also shown for comparison.

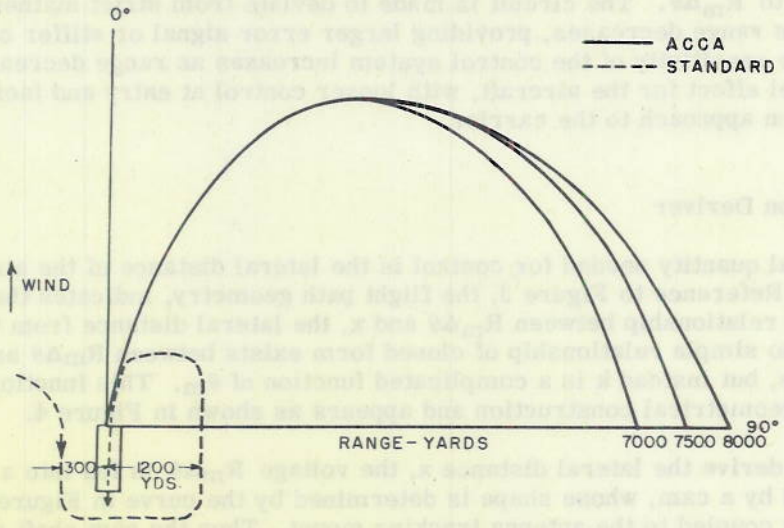

Figure 2 - Flight patterns

At the flight path entry point, a 1000-yard-wide gate is provided. That is, a family of flight paths is generated which intersect the 90° azimuth at ranges of from 7,000 to 8,000 yards. All of these paths coalesce to a single flight path at about 4,000 yards. Thus, as soon as radar tracking is initiated, an "initial closure" circuit is energized, which selects the flight path passing through the position of the aircraft at capture. The effect is that of tieing one end of the flight path to the aircraft entering the control phase. The time required for path selection is in the order of 1/2 second and after a period of 2 to 5 seconds, the initial closure circuit is deenergized and the selected path for the aircraft under control is frozen.

The radar site is not coincident with the flight deck center line, so that at ranges smaller than 400 yards the resulting parallax is very severe and correction must be included to pass the flight course down the carrier center line. This is accomplished by means of a final-approach circuit which remains inoperative at ranges in excess of 400 yards but is switched in by the range voltage when the aircraft reaches the 400-yard point.

The Comparator

The computed azimuth, the output of the flight path deriver, is fed into the comparator, where it is compared with the azimuth of the aircraft as measured by the radar. The comparator is a differencing circuit, which converts the difference between two d-c voltages into a 1000-cps square wave, whose amplitude is proportional to $\Delta\theta = \theta_c - \theta_m$, the difference between computed and measured azimuth, and whose phase is either 0° or 180° depending on whether $\theta_c - \theta_m$ is greater than or less than zero.

The Range Multiplier

The output of the comparator, $\theta_c - \theta_m$ is fed into the range multiplier, and multiplied by a voltage proportional to measured range. The resultant output then is a voltage that

is proportional to $R_m\Delta\theta$. The circuit is made to deviate from strict mathematical multiplication as range decreases, providing larger error signal or stiffer control at short range. Thus the sensitivity of the control system increases as range decreases. This provides a funnel effect for the aircraft, with looser control at entry and increasingly tighter control on approach to the carrier.

Lateral Deviation Deriver

The physical quantity needed for control is the lateral distance of the aircraft from the flight path. Reference to Figure 3, the flight path geometry, indicates that there is some functional relationship between $R_m\Delta\theta$ and x, the lateral distance from the path. Unfortunately, no simple relationship of closed form exists between $R_m\Delta\theta$ and x throughout the flight course, but instead k is a complicated function of θ_m. This function of θ_m was established by geometrical construction and appears as shown in Figure 4.

In order to derive the lateral distance x, the voltage $R_m\Delta\theta$ is fed into a linear potentiometer actuated by a cam, whose shape is determined by the curve in Figure 4. The cam shaft is directly coupled to the antenna tracking mount. Thus the cam shaft position is always directly related to θ_m, the measured azimuth and the potentiometer output is proportional to $k(\theta)R_m\Delta\theta$. A photograph of the lateral deviation deriver is shown in Figure 5.

Equalization Network

In order to provide stable control, with relatively rapid close-out of transients and with relatively low accelerations imposed on the aircraft, it was found necessary to use proportional plus derivative control. A detailed discussion of the problems involved and the result obtainable follow in the section of this report under dynamics. Functionally, it is necessary to provide an error signal which is proportional to the sum of the lateral deviation of the aircraft and the time derivative of the lateral deviation. Thus, the error signal should be

$$E_S = k_1 x + k_2 \dot{x}. \qquad (1)$$

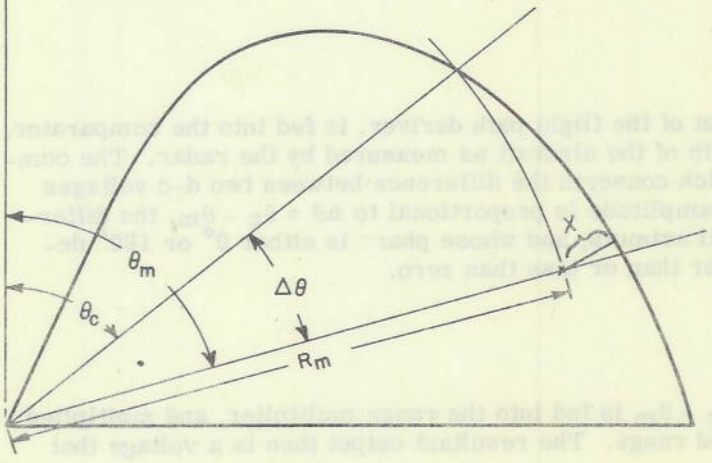

Figure 3 - Flight path geometry

Illustrating functional relation between x the perpendicular distance of the aircraft from the derived path and $R_m\Delta\theta$

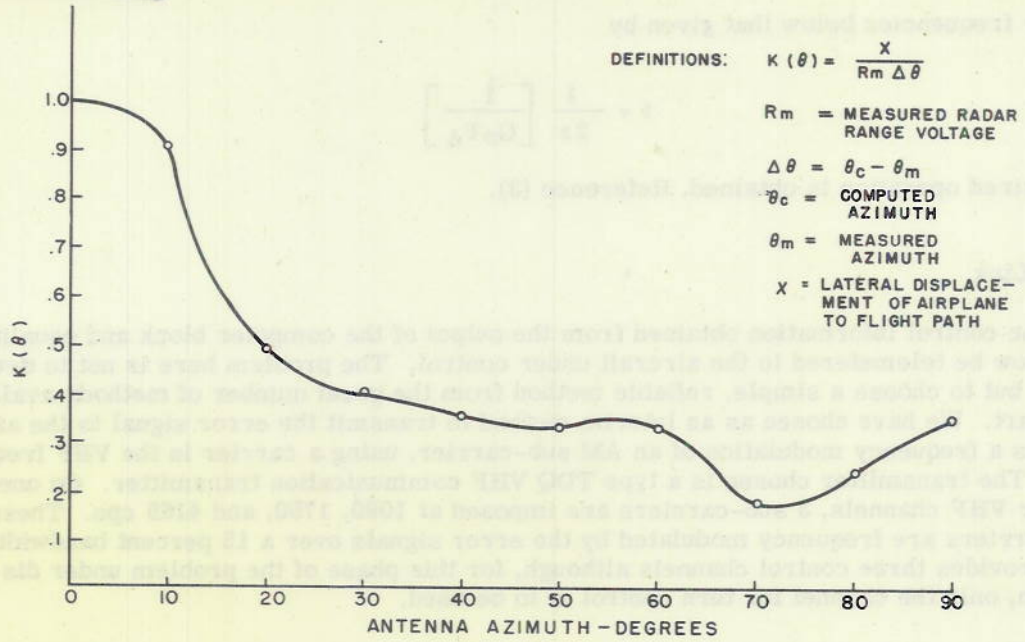

Figure 4 - K(θ) vs. antenna azimuth curve (D_1 deriver output)

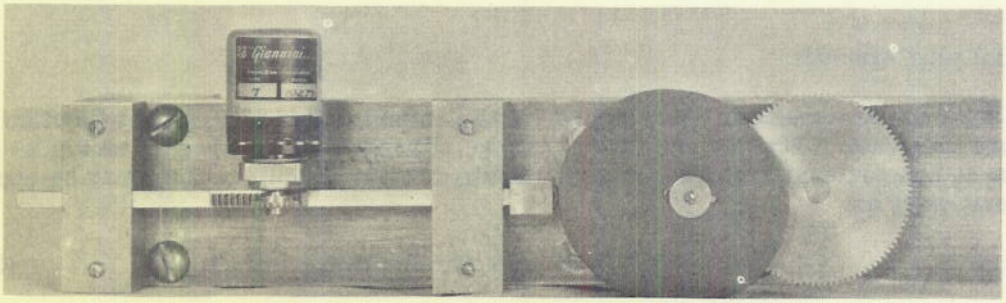

Figure 5 - Lateral deviation deriver

Since x appears as a d-c voltage, it is relatively easy to derive such an error signal by means of a simple equalization network as shown below in Figure 6.

The transfer function of such a network is

$$Y(p) = \frac{G_O (T_A p + 1)}{G_O T_A p + 1}, \qquad (2)$$

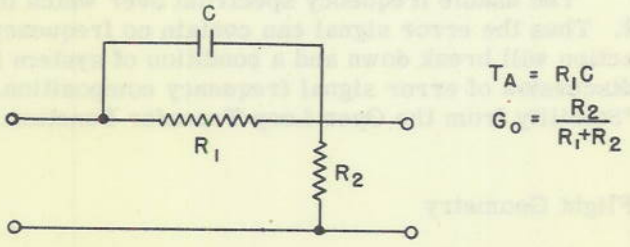

Figure 6

and for frequencies below that given by

$$f = \frac{1}{2\pi}\left[\frac{1}{G_0 T_A}\right]$$

the desired operation is obtained, Reference (3).

Radio Link

The control information obtained from the output of the computer block and equalizer must now be telemetered to the aircraft under control. The problem here is not to devise a way, but to choose a simple, reliable method from the great number of methods available to the art. We have chosen as an interim method to transmit the error signal to the aircraft as a frequency modulation of an AM sub-carrier, using a carrier in the VHF frequency band. The transmitter chosen is a type TDQ VHF communication transmitter. On one of its four VHF channels, 3 sub-carriers are imposed at 1090, 1790, and 4165 cps. These sub-carriers are frequency modulated by the error signals over a 15 percent bandwidth. This provides three control channels although, for this phase of the problem under discussion, only the channel for turn control is to be used.

In the aircraft, the three sub-carriers are filtered out separately and the frequency modulated intelligence converted back to its original error signal d-c voltage form by means of audio-frequency discriminators. Finally, the error signal is converted to the required form necessary to actuate the autopilot by means of an autopilot coupler.

Autopilot plus Aircraft

It has been assumed that the response of the autopilot plus aircraft combination is that of a pure integrator. That is, the rate of change of heading of the aircraft autopilot combination is proportional to the error signal applied to the autopilot. This may be expressed mathematically as

$$\beta \text{ (the heading of the aircraft)} = \int E_S dt. \qquad (3)$$

Aircraft plus autopilot response has been discussed in articles by Greenberg (4), Titus (5), and Gaylord (6). An attempt to verify experimentally true integrator action has been made by Radio Division III of this Laboratory, and a detailed discussion of this result will appear in a report soon to be published. Preliminary data seem to support the assumption that integrator action will result over a limited frequency spectrum.

The usable frequency spectrum over which integrator action results is shown in Figure 7. Thus the error signal can contain no frequency component in excess of w_c or integrator action will break down and a condition of system instability may result. For more detailed discussion of error signal frequency composition, refer to the section of this report entitled "Stability from the Open Loop Transfer Function."

Flight Geometry

As discussed above, the response of the aircraft autopilot combination to an error signal is a time rate of change of heading. The radar determination is in the form of

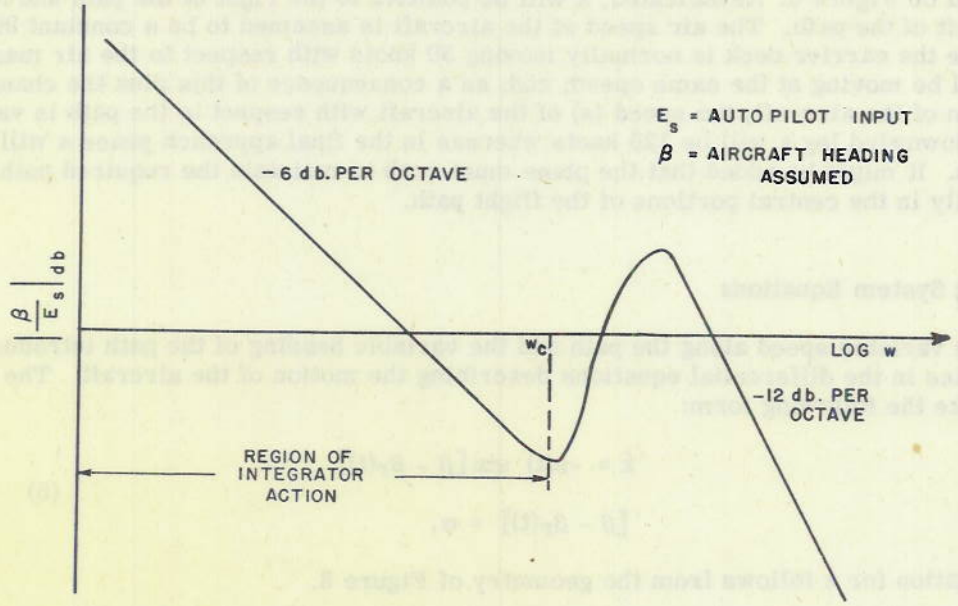

Figure 7 - Aircraft plus autopilot response to sinusoidal forcing function

position coordinate information. Thus, the flight geometry becomes a block in the servo loop. The function of the geometry block is to convert the aircraft heading into position of the aircraft. The nature of this block can better be understood by reference to the analytical discussion of the flight geometry appearing in the body of this report below.

DYNAMICS

Geometry and Sign Convention

In Figure 8 are illustrated the angular and linear relationships of the aircraft in following the derived path into the carrier. Line EF is parallel to the fore-aft line of the carrier. β, the aircraft heading, as well as β_r, the heading of the derived path, are measured from EF. β is positive when to the left of EF and negative when to the right of EF. β_r is always positive since path entry is not exactly perpendicular to EC. The algebraic difference of β and β_r is the instantaneous heading error of the plane:

$$\alpha = (\beta - \beta_r). \qquad (4)$$

The position error x is defined as the perpendicular displacement of the plane from the derived path as is

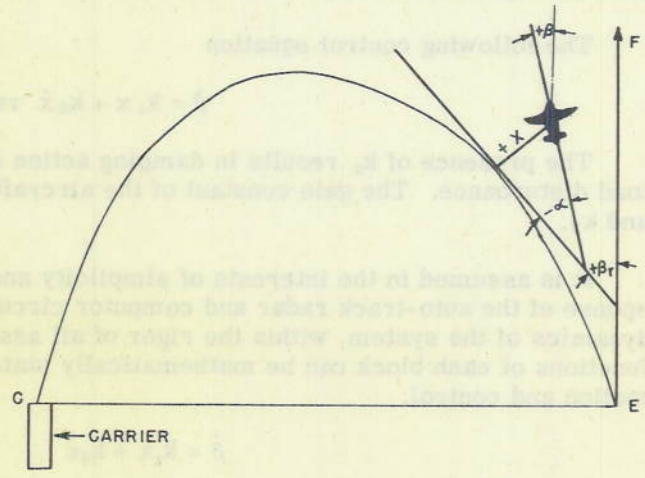

Figure 8 - Flight path geometry and sign convention

indicated on Figure 8. As indicated, x will be positive to the right of the path and negative to the left of the path. The air speed of the aircraft is assumed to be a constant 90 knots but since the carrier deck is normally moving 30 knots with respect to the air mass, the path will be moving at the same speed; and, as a consequence of this plus the changing direction of the aircraft, the speed (s) of the aircraft with respect to the path is variable. On the downwind leg s will be 120 knots whereas in the final approach phase s will approach 60 knots. It might be added that the plane must crab to maintain the required path heading, especially in the central portions of the flight path.

Defining System Equations

The variable speed along the path and the variable heading of the path introduce non-linearities in the differential equations describing the motion of the aircraft. The equations take the following form:

$$\dot{x} = -s(t) \sin[\beta - \beta_r(t)]$$
$$[\beta - \beta_r(t)] = \alpha. \tag{5}$$

The equation for $\dot{x}$ follows from the geometry of Figure 8.

β_r will vary from a few degrees at the path entry point to 180° at touchdown. The variations are a monotonically increasing function of time which is apparent from an examination of the flight path. $\dot{x}$ is the rate at which the position error lateral to the path is varying.

The equation of control results from the proportional plus derivative composition of the error signal and heading response characteristics of the aircraft. The system requires a portion of the error signal be time rate of change of x and hence x plus $\dot{x}$ are used to control the aircraft. It is assumed that an aircraft autopilot combination turns in the yaw axis at a rate proportional to the error signal within a wide range of turning rates (see section on "Autopilot plus Aircraft"). Hence the response of the aircraft is assumed to be the integral of the error signal fed it.

The following control equation

$$\dot{\beta} = k_1 x + k_2 \dot{x} \text{ results.} \tag{6}$$

The presence of k_2 results in damping action on desired state disturbances and on load disturbance. The gain constant of the aircraft plus autopilot is contained within k_1 and k_2.

It is assumed in the interests of simplicity and for preliminary analysis that the response of the auto-track radar and computor circuits is not a function of frequency. The dynamics of the system, within the rigor of all assumptions made regarding the transfer functions of each block can be mathematically stated by a combination of equations of motion and control:

$$\dot{\beta} = k_1 x + k_2 \dot{x}$$
$$\dot{x} = -s(t) \sin[\beta - \beta_r(t)]. \tag{7}$$

Solution of System Equations

The differential equations are not subject to standard servo analysis because of the nonlinearities existing in the system. It is possible to make the equations amenable to servo techniques with the aid of certain linearizing assumptions. In order to justify such assumptions, however, a solution was obtained for the nonlinear case with the aid of a REAC Analog computor. Solutions were obtained for x and $\dot{\beta}$ for various choices of k_1 and k_2 assuming various heading errors out to and including 45^0. These solutions were obtained with x(0) = 0 which is a consequence of the initial servo closure circuit. The system solutions revealed that:

(1) In no case would the system be more than marginally unstable either for $k_2 = 0$ or for system gain very small (within the assumptions made).

(2) An optimum choice of k_2 and k_1 could be made from considerations of acceleration, closure time, and oscillatory motion.

(3) A comparison of the analog computor solution with that obtained for the linear case—s constant, $\beta_r(t) = 0$ and $\sin[\beta - \beta_r] = \alpha$—shows for $\alpha(0) = \pm 25^0$, the two solutions do not differ from each other in amplitude or frequency by more than 10 percent.

(4) The solution is of a damped oscillatory nature.

Figures 9 and 10 show solutions of x and β plotted by an analog computor for the nonlinear case. The values of k_1 and k_2 were chosen to allow for a reasonable closure time for the transient arising out of an initial heading error of -45^0. $\beta_r(t)$ and s(t) were provided to the computor graphically as functions of time in effecting a solution by computor techniques.

From (1) in the list above it is evident that the correct type of control has been chosen. From (2) above it was possible to choose k_1 and k_2 so as to make transient closure time 20 seconds with peak accelerations total within 1.64 g for $\alpha(0) = 45^0$. Most important from (3) above it was evident that the system could be made subject to servo-mechanism analysis within the excursion of parameters of interest.

Servo System Analysis

It becomes of interest to set up the system as a servoblock to learn more about system stability as it relates to the transfer functions of the auto-track radar, the computor, and the r-f telemetering link (see Figure 1). The transfer characteristics of these blocks, and in particular their time lags, have not yet been determined.

The system with assumptions of unity transfer functions for the auto-track radar, the computor, and the r-f telemetering link can be set up as shown in Figure 11, where

v(p) - Desired position of aircraft in LaPlace transform

r(p) - Regulated position of aircraft in LaPlace transform

x(p) - Position error in LaPlace transform

l(p) - Load disturbance on the aircraft = $-\alpha_0/p$

w_{01}/p - Transfer function for aircraft autopilot combination

s_m/p - Transfer function for flight path geometry

$G_0(1+T_Ap)$ - Transfer function for the lead network

$E_S(p)$ - LaPlace transform of the error signal

$\alpha(p)$ - LaPlace transform of the instantaneous heading error

s - A maximum value since x(t) contains broadest frequency composition required of computor networks during the initial transient when the relative speed is a maximum.

Thus the error response to an initial step heading error, which is in the nature of a load disturbance is

$$x(p) = \frac{s_m \alpha_0/p^2}{1 + \frac{w_{01} s_m G_0}{p^2}(1 + T_Ap)} = \frac{s_m \alpha_0}{p^2 + w_{01}sG_0T_Ap + w_{01}sG_0} \quad (8)$$

If we assume w_{01} contained within G_0 as was done for the differential equation we get

$$x(p) = \frac{s_m \alpha_0}{p^2 + s_mG_0T_Ap + s_mG_0} = \frac{s_m \alpha_0}{p^2 + s_mk_2p + s_mk_1} \quad (9)$$

hence

$$x(t) = \frac{2s_m \alpha_0}{\sqrt{s_m^2k_2^2 - 4s_mk_1}} e^{-s_mk_2t/2} \sinh \frac{\sqrt{s_m^2k_2^2 - 4s_mk_1}}{a} t. \quad (10)$$

This represents the displacement resulting from an initial heading error of $-\alpha_0$. The solution becomes a damped sinusoid according to whether or not the radical is imaginary which confirms the results of the computor work.

The servo analysis approach is to study system performance in terms of frequency response of the open loop transfer function gh(p) without ever reverting to the time domain, though actually time domain performance is the physical phenomenon of interest. It might be added that Equation (10) can be obtained by linearizing the equations of the system and solving by LaPlace transform methods.

Stability from the Open Loop Transfer Function

Reference to Figure 11 of the over-all block diagram in servo form, along with assumptions of unity transfer functions for auto-track radar and computor, shows that the open loop transfer function is:

$$gh(p) = \frac{G_0s_m}{p^2}\left(\frac{1 + T_Ap}{1 + G_0T_Ap}\right). \quad (11)$$

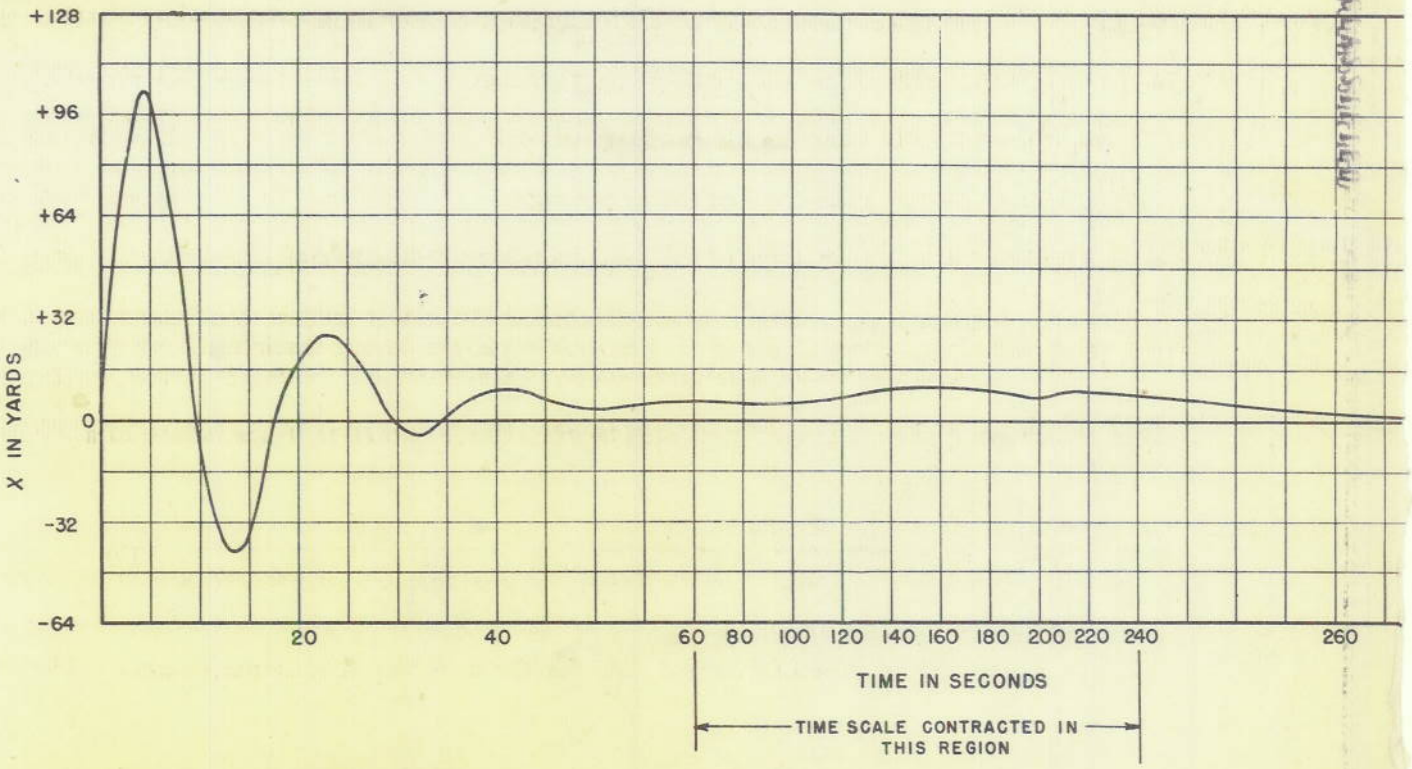

Figure 9 - Plot of x vs. t

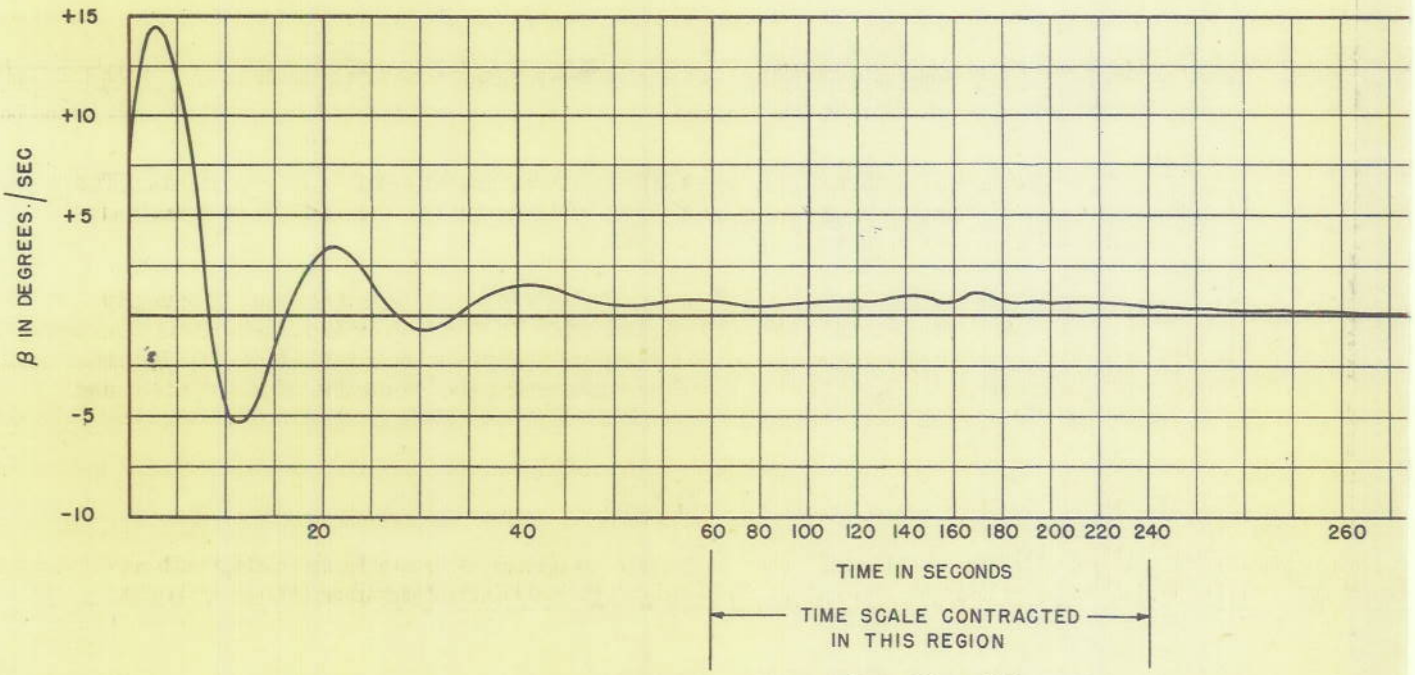

Figure 10 - Plot of β vs. t

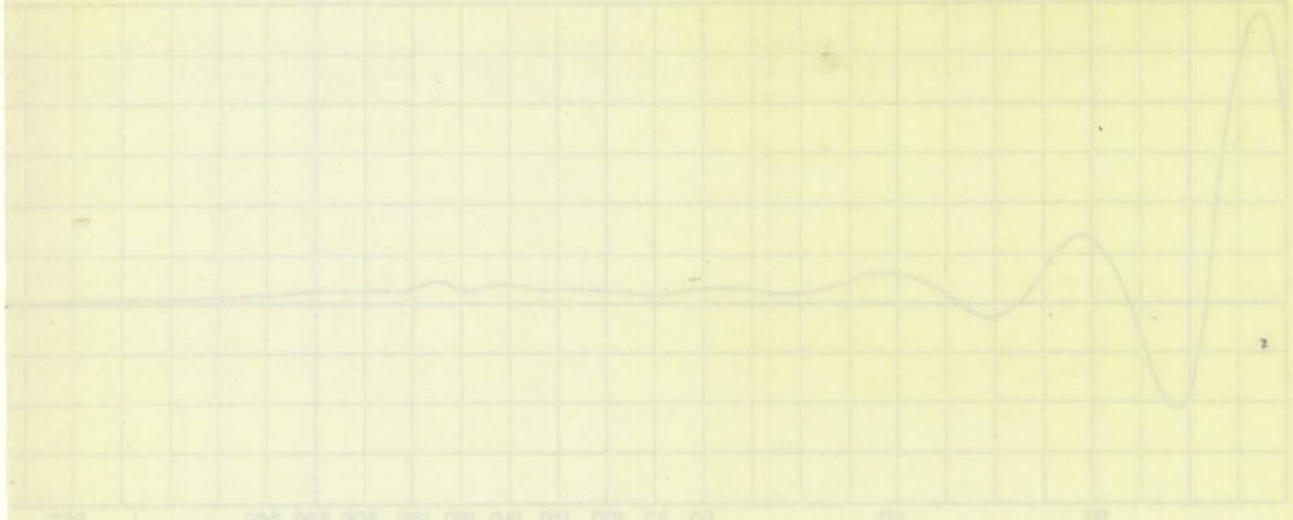

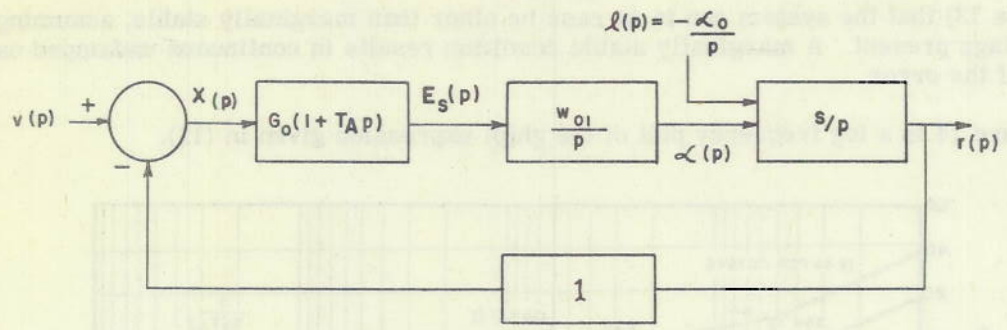

Figure 11 - ACCA servo loop

The Nyquist diagram for the transfer locus of gh(p) appears in Figure 12. If one assumes that the proportional plus derivative property of the lead network holds throughout the frequency composition of x(t) the diagram for the transfer locus simplifies to Figure 13. Assumptions of the proportional plus derivative property of the lead network can be satisfied by appropriate design. This means that $G_0T_Ap \ll 1$ for all frequencies transmitted by the equalization network where

$$gh(p) = \frac{G_0 s_m}{p^2}\left(1 + T_A p\right) . \qquad (12)$$

For the under damped case of interest, gain crossover occurs at $\omega = .707$ where $\omega = wT_A$ and $w = .384$ rad's/sec. The phase margin at gain crossover is 35^0. It is apparent from the diagram that as gain is increased, the phase margin increases as does the frequency of gain crossover. The result is that the system becomes less oscillatory with progressively more damping. As the gain is increased still further critical damping results after which the system becomes over damped, ceases to oscillate, and becomes sluggish.

Decreasing the gain results in higher period oscillations with less and less damping. The choice of gain level was made to result in just one over shoot in the error within radar range resolution for operational reasons.

The condition for critical damping is that gain crossover occurs at $\omega = 4.18$ or $w = 2.27$ rad's/sec with 76^0 phase margin. It is evident from the Nyquist diagram (either Figure 12

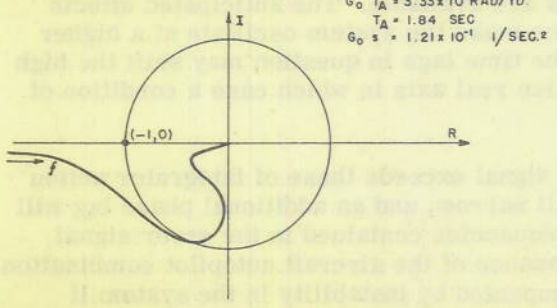

Figure 12 - Transfer locus of gh

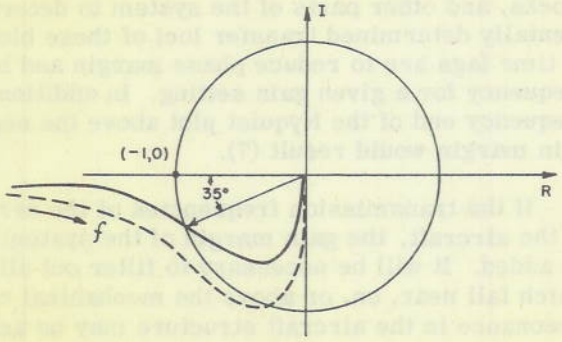

Figure 13 - Transfer locus of gh assuming proportional plus derivative equalization throughout the frequency spectrum

or Figure 13) that the system can in no case be other than marginally stable, assuming no time lags present. A marginally stable condition results in continuous undamped oscillations of the error.

Figure 14 is a log frequency plot of the gh(p) expression given in (11).

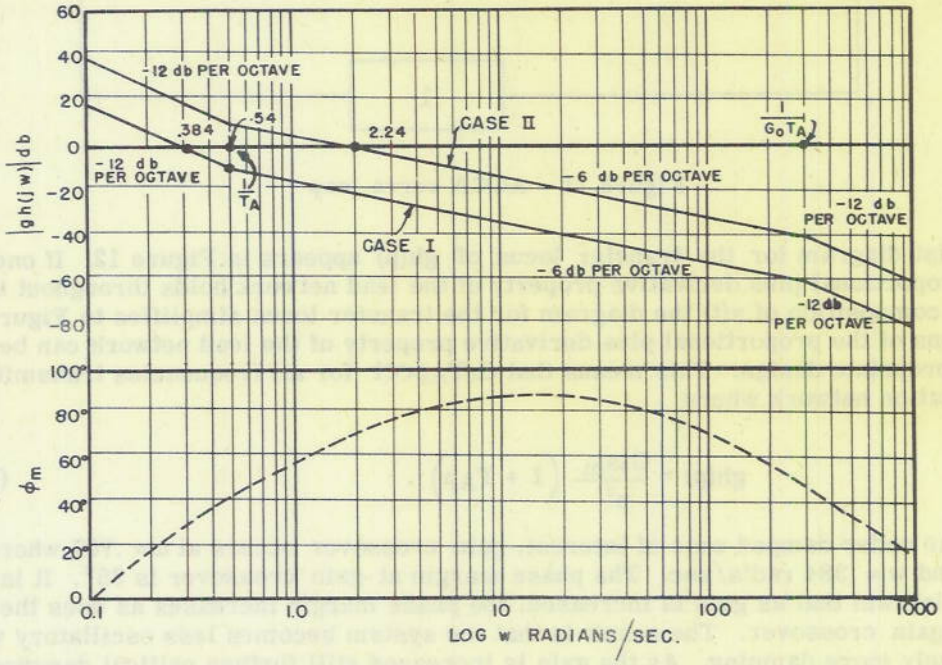

Figure 14 - Log frequency plot of transfer locus
Case I - Path of interest
Case II - Critically damped case

The log frequency plots in Figure 14 which are complimentary to the Nyquist diagram present another picture of the variation of the gh(p) product shown in Figure 12 and hence, the key to servo performance. Figure 14 also illustrates the variation in phase margin ϕ_m. with frequency.

The servo approach will be extended to include the time constants in radar, computor blocks, and other parts of the system to determine their effect on stability when experimentally determined transfer loci of these blocks are available. The anticipated effects of time lags are to reduce phase margin and hence make the system oscillate at a higher frequency for a given gain setting. In addition, the time lags in question may shift the high frequency end of the Nyquist plot above the negative real axis in which case a condition of gain margin would result (7).

If the transmission frequencies of the error signal exceeds those of integrator action of the aircraft, the gain margin of the system will narrow, and an additional phase lag will be added. It will be necessary to filter out all frequencies contained in the error signal which fall near, on, or above the mechanical resonance of the aircraft autopilot combination. Resonance in the aircraft structure may be accompanied by instability in the system if phase margin and gain margin requirements are no longer met.

Fourier Transform Analysis

There exists a variety of random time functions generated at different points in the control loop as a consequence of control. These random functions result from vertical as well as horizontal motions of the aircraft and carrier deck. In order to make a valid prediction of the performance, especially the stability of a closed loop system, it is necessary to have a knowledge of the frequency composition of the time functions to be passed (transferred) by each of the loop blocks in question.

As a result of these conditions the following time functions were Fourier transformed:

R(t) - Range from 8,000 to 150 yards

$\theta(t)$ - Angular measure from 90° to 0°

$\dot{\beta}(t)$ - Time rate of absolute heading change

x(t) - Lateral path displacement

It may be added that these functions do not comprise a complete list of the frequency studies necessary but deal solely with disturbances acting on control in the turn axis.

The time functions were obtained for the case of a 45° entry heading error as representative of an extreme step error. The defining relation in question is

$$|G(jw)|_{db} = \frac{1}{2\pi}\left|\int_0^{300\ \text{sec}} e^{-jwt} f(t)\ dt\right| . \qquad (13)$$

The zero-db reference chosen was the natural period of damped oscillation for $\dot{\beta}(t)$ and x(t). While a median value was chosen for R(t) and $\theta(t)$, the 300-sec interval of integration is the time necessary for the aircraft to traverse the derived path.

The curves of the frequency content versus log w are illustrated in Figures 15, 16, 17, and 18. The frequency components 40 db down or more from the established zero-db reference are to be eliminated by appropriate filtering. The auto-track radar will be required to pass $|R(jw)|$ and $|\theta(jw)|$ in the range and azimuth tracking circuits respectively.

The highest frequency component contained in $|\dot{\beta}(jw)|$ cannot exceed the frequency at which the aircraft plus autopilot integrator action breaks down, which may result in system instability. From Figure 17 the amplitude of frequencies 5 radians/sec are at least 40 db down from the chosen zero-db reference. Certain classes of aircraft have integrator properties from zero to 6 to 9 radians/sec. Hence, the control stiffness and consequent initially generated transient appears compatible with the integrator requirement. The equalization network must maintain its derivative properties beyond the cut-off of $|x(jw)|$; this means $w_{co} \leq 1/G_0T_A$ as may be seen from the section on equalization network. The arbitrarily defined cut-off frequency of x(jw) appears in Figure 18.

Radar Tracking Characteristics

No deleterious time lags are anticipated in the radar tracking circuits within the frequency composition of the ACCA servo variables. This belief arises out of two considerations.

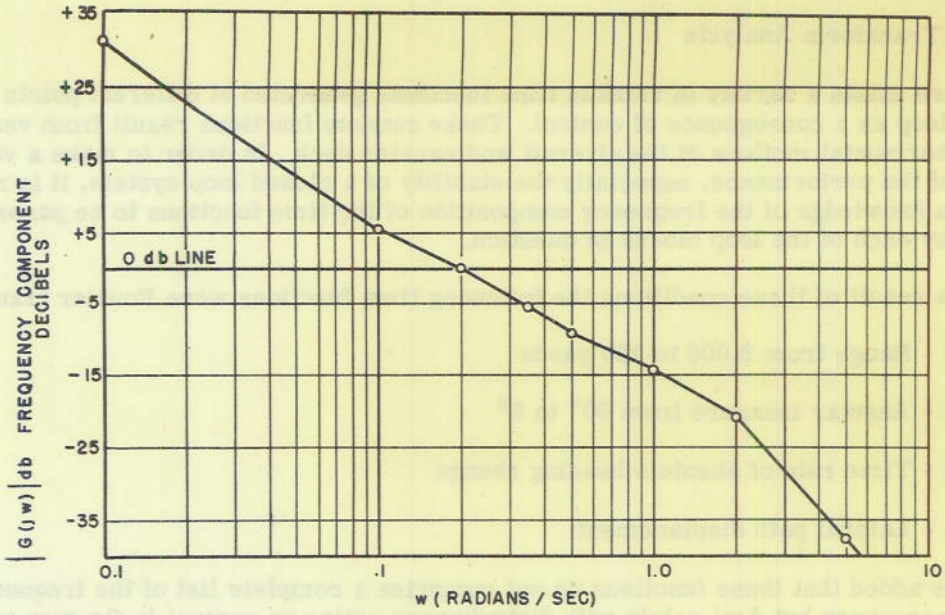

Figure 15 - R(jw) - Frequency spectrum of R(t), $\alpha(0) = 45^0$, $x(0) = 0$

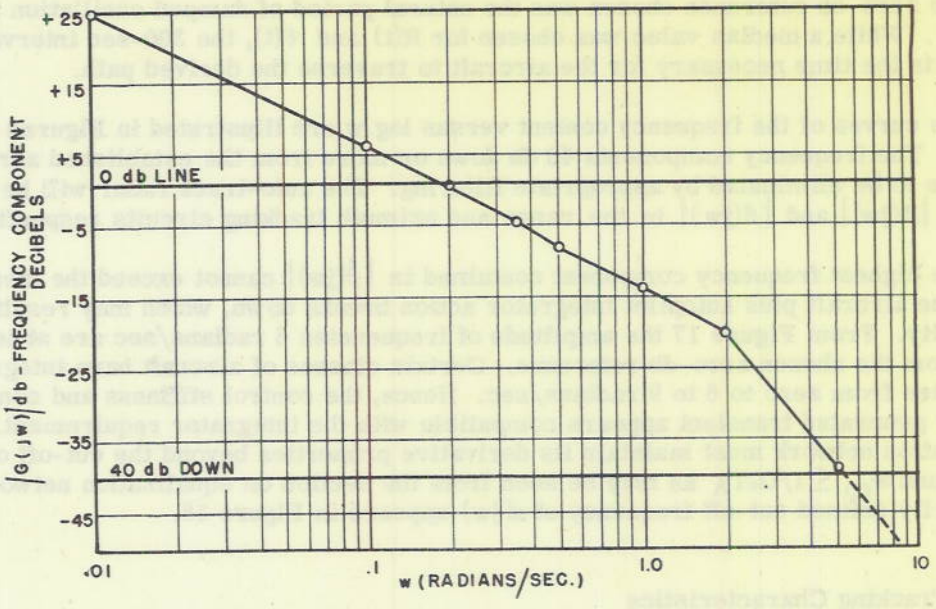

Figure 16 - θ(jw) - Frequency spectrum of θ(t), $\alpha(0) = 45^0$, $x(0) = 0$

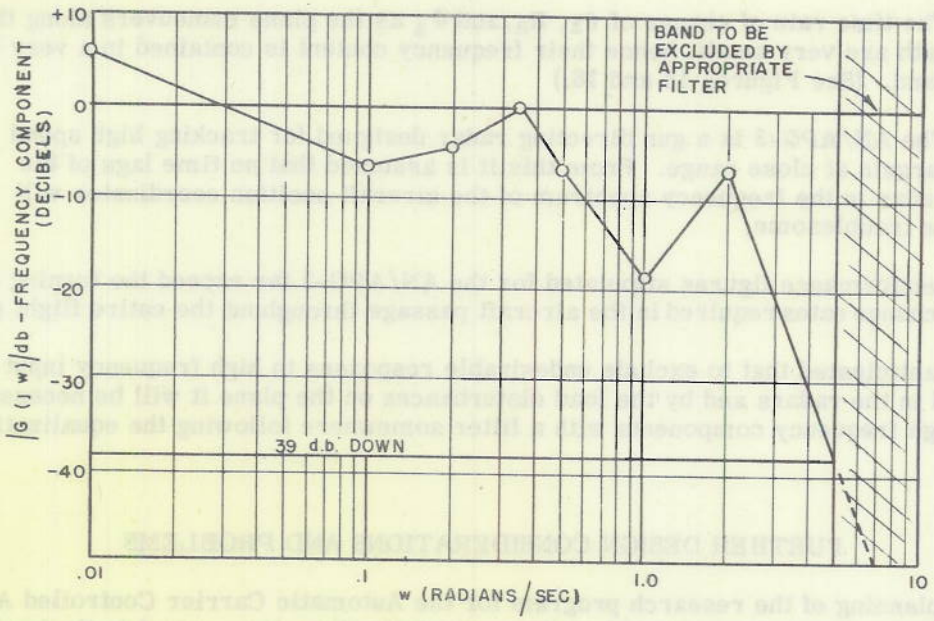

Figure 17 - $\dot{\beta}(jw)$ - Frequency spectrum of $\dot{\beta}(t)$, $\alpha(0) = 45^0$, $x(0) = 0$

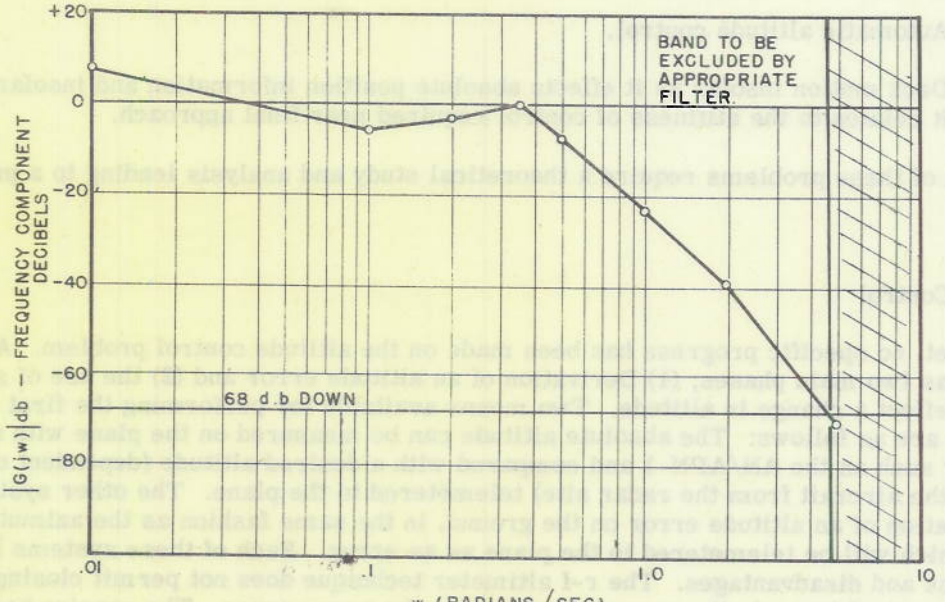

Figure 18 - x(jw) - Frequency spectrum of x(t), $\alpha(0) = 45^0$, $x(0) = 0$

CONFIDENTIAL

(1) The time rate of change of θ_a, R_a, and Φ_a as the plane maneuvers along the path are very small, hence their frequency content is contained in a very low band. (See Figures 15 and 16.)

(2) The AN/APG-3 is a gun directing radar designed for tracking high speed targets at close range. From this it is assumed that no time lags of the radar in the frequency spectrum of the aircraft position coordinates will be troublesome.

The performance figures stipulated for the AN/APG-3 far exceed the turning rates and the range change rates required in the aircraft passage throughout the entire flight path.

It is anticipated that to exclude undesirable responses to high frequency input noise generated in the radars and by the load disturbances on the plane it will be necessary to bypass high frequency components with a filter somewhere following the equalization channel.

FURTHER DESIGN CONSIDERATIONS AND PROBLEMS

The planning of the research program for the Automatic Carrier Controlled Approach (ACCA) system has been conducted on the supposition that when control in the horizontal plane has been achieved the knowledge of design and techniques gained thereby will provide a basis for design of control systems for altitude and attitude control.

Several important considerations remain to be investigated before anything resembling a completely automatic system can be proposed in detail. Two of the more evident problems remaining are:

(1) Automatic altitude control,

(2) Deck motion insofar as it effects absolute position information and insofar as it relates to the stiffness of control required near final approach.

Each of these problems require a theoretical study and analysis leading to a practical solution.

Altitude Control

As yet, no specific progress has been made on the altitude control problem. Altitude control has two main phases; (1) Derivation of an altitude error and (2) the use of said error to effect a change in altitude. Two means available for performing the first of these functions are as follows: The absolute altitude can be measured on the plane with an r-f altimeter such as the AN/APN-1 and compared with a desired altitude (dependent on the range of the aircraft from the radar site) telemetered to the plane. The other system is the derivation of an altitude error on the ground, in the same fashion as the azimuth angular error, which will be telemetered to the plane as an error. Each of these systems has its limitations and disadvantages. The r-f altimeter technique does not permit closing the elevation control loop via the ground computor in the servo sense. The carrier base would not be aware of failure of the aircraft altimeter or associated computor networks. Generation of altitude error on the ground presents difficulties by reason of (1) poor percentage accuracy at low altitude, (2) the presence of sea returns and multiple path transmission, and (3) instability of the radar platform.

The manner in which an altitude error is used depends in part on aerodynamic considerations. This stems from the fact that, for a system such as that proposed in ACCA, while maintaining a constant air speed, a change in altitude requires a change in attitude coordinated with a change in power settings on the aircraft engines. Both Minneapolis-Honeywell Regulator Co. under the auspices of Special Devices Center USN and Bendix Corporation have been and are currently working on the altitude control problem. One approach to the problem has been to coordinate the autopilot with an angle-of-attack sensing device to maintain the requisite aircraft performance while effecting an altitude change. The Automatic Ground Controlled Approach system has achieved elevation control without coordinated throttle adjustment by using adequate gain in the elevation control loop. A thorough study will be made of available techniques and their suitability to the engineering and operational requirements of ACCA to determine the best approach to this problem.

The following presents a detailed functional proposal of the two available types of altitude control previously mentioned.

Automatic Altitude Control Employing Radar Height Finding. Basing an altitude control channel on height finding data from a carrier-sited radar, we may propose the control system shown in block form in Figure 19.

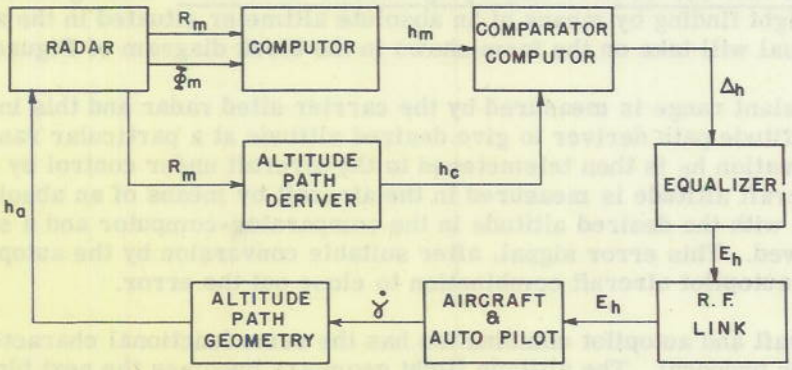

Figure 19 - Altitude control employing radar height finding

Aircraft slant range and elevation data are gathered by the carrier sited radar. The measured range voltage feeds the altitude path deriver whose output is a voltage proportional to the desired altitude, h_c. Slant range and elevation data in combination are converted to aircraft altitude by means of a computor. From geometrical considerations, it is evident that the computed altitude h_m is proportional to the product of slant range times the sine of the radar elevation angle. Gearing a sine potentiometer to the radar antenna elevation drive and feeding slant range into this potentiometer will give the computed altitude output, h_m. The generated desired altitude is compared with the computed measured altitude h_m and a suitable error signal E_h derived.

The error signal used in controlling aircraft altitude position is telemetered to the aircraft under control by means of an r-f link. The autopilot coupler transforms the error signal to the desired form which feeds the autopilot and aircraft combination to close out the error. The aircraft and autopilot combination is assumed to act as a pure integrator in the pitch axis in substantially the same manner as in the turn axis. The altitude flight

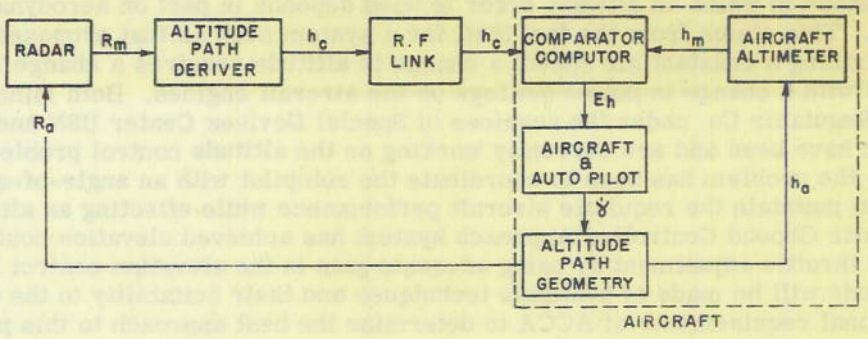

Figure 20 - Altitude control employing airborne altimeter

geometry which converts the aircraft output, $\dot{\gamma}$, the time rate of change of aircraft angle of attack, into corrected altitude becomes the next block in the servo loop. The servo loop is then closed by means of the radar.

Automatic Altitude Control Employing a Radio Altimeter. Basing an altitude control channel on height finding by means of an absolute altimeter situated in the aircraft, the system proposal will take on the form shown in the block diagram of Figure 20.

Aircraft slant range is measured by the carrier sited radar and this information is fed into the altitude path deriver to give desired altitude at a particular range. The desired altitude information h_c is then telemetered to the aircraft under control by means of an r-f link. Aircraft altitude is measured in the aircraft by means of an absolute altimeter and compared with the desired altitude in the comparator-computor and a suitable error signal is derived. This error signal, after suitable conversion by the autopilot coupler, is fed into the autopilot aircraft combination to close out the error.

The aircraft and autopilot combination has the same functional character as outlined in the previous proposal. The altitude flight geometry becomes the next block in the servo loop. The loop is then closed by the absolute altimeter in its altitude gathering role.

Deck Motion

In general the deck is a rather unstable landing platform. This has an important bearing on the design and system component requirements of an ACCA. If the ACCA reaches a satisfactory completion, efforts will be made to extend the control region to touchdown. In such a case deck motion studies and appropriate system compensation for such motions will become of even greater importance.

The motions of the fan tail of a carrier are resolvable into four components, three rotational and one translational. Of these four motions only two merit consideration insofar as control in the last phases of descent are concerned. The four motion components mentioned are yaw, roll, pitch, and heave. The effects of yaw on the control problem have been discussed under radar. Roll motions on the carrier are of importance only in the last phases of landing under the supervision of the LSO and hence do not enter into the design requirements of an automatic approach system.

If the heave motion of the ship under all conditions acceptable for landing operations is less than the height resolution of the ship mounted radar, it can be regarded as an error

less than system resolution and hence requires no further consideration. If on the other hand heave motion becomes two or more times the height resolution of the system, it will be necessary by accelerometer means or otherwise to abstract the heave motion of the ship from its over-all motion. The heave motion will then be used as an additional error control on the aircrafts altitude. The heave control as it relates to the aircrafts altitude will take either of two forms. If the heave motion of the carrier is large, the voltage generated as being representative of it will be fed into a prediction network whose function is to generate a voltage which predicts the future value of the heave at a time Δt later. This will in turn permit smoothing correction of the aircrafts altitude position to permit coincidence with ships heave motion in the neighborhood of touchdown. If experimental observation under a variety of operating conditions prove heave motions to be of more moderate proportions, they may be range sensitized in such a way that near touchdown a 1-to-1 correspondence between carrier deck position and aircraft altitude position will result. A time frequency domain study of heave motions will be necessary before a specific engineering solution to these problems can be developed including response time requirements in the elevation control loop.

The pitch motions of the carrier are highly important insofar as any automatic approach control are concerned. The same height resolution considerations that apply to heave also apply to pitch. In general it is anticipated that pitch motion will exceed height resolution in the approach phase. The present intention is to generate voltages proportional to the pitch motion and to use prediction networks for smooth correction of the altitude control signals.

It is hoped that the prediction voltage will permit smooth asymptotic elevation control closing to coincide with ship motion near touchdown.

FUTURE PROGRAM

This report has outlined the major design considerations that have gone into the proposed NRL ACCA system. Subsequent reports will cover the detailed circuitry involved in the components of the system as they have been built up for the experimental program.

However, it is not intended that this report indicate the full scope of the activity in the all-weather flying program of NRL. Rather the ACCA system described will be used as a research tool toward the investigation of broader problems in that program. The completion of the automatic approach equipment will signal the start of investigation toward fully automatic landing operation aboard carriers. It will also allow the consideration of more than one aircraft in the control zone at one time with the attendent problems of traffic feed-in and speed and/or path-length variation for interval control. The wave-off problem will be studied from technical and operational viewpoints in such a way that reliable and fail-safe provisions are retained. The altitude control channel will be instrumented in manner satisfying the requirements discussed in the text of this report. The ship-to-air data link will be investigated for a permanent and efficient solution in contrast to the interim method which is being used at the present time.

Finally, it is recognized that a major problem in coordination exists. Not only must such a system be consistent within itself insofar as it provides an operationally acceptable solution to a fleet problem, but it must also be compatible, technically and operationally, with all electronic gear requisite to carrier operations. This means, for example, that the data transmission link must be coordinated with a link used for air defense, traffic control, short distance navigation, etc. Further, the use of ACCA must be operationally compatible with the other essential carrier functions, such as the Combat Information Center.

* * *

REFERENCES

(1) Brodzinsky, A., "Recommended Research Program for Carrier All-Weather Flying," NRL Report R-3458 (Confidential), 27 April 1949

(2) "PB-10 Automatic Pilot with Flight Path Control" Bendix Aviation Corporation Publication No. 73-21A (Unclassified); also Gilfillan Brothers Inc., Los Angeles, California, Report No. 340-36, "Automatic GCA System" (Restricted), 15 May 1949

(3) For more detailed discussion of these and other equalization networks see James, H. M., Nichols, N. B., and Phillips, R. S., "Theory of Servo Mechanisms," McGraw-Hill, New York, 1947.

(4) Greenberg, Harry, "Frequency-Response Method for Determination of Dynamic Stability Characteristics of Airplanes with Automatic Controls," NACA Report No. 882 (Unclassified), 1947

(5) Titus, J. W., "Response of an Airframe to Sinusoidal Wing Flap Deflection," NRL Report No. R-3253 (Confidential), 5 March 1948

(6) Gaylord, R. E., "Development of an Aircraft Control System," NRL Report R-3108, Appendix II, of Lark-Wasp Guided Missile Seminar (Confidential), April 1947

(7) Ahrendt, W. R., and Taplin, J. F., "Automatic Regulation," Ahrendt and Taplin, Washington, D. C., 1947

* * *

APPENDIX
Pertinent Observations Made During Operation PORTREX of Carrier Aircraft Landings as Applied to ACCA

H. W. Chitty and Kenneth L. Huntley

INTRODUCTION

A group of NRL personnel (see appended list) were present, as observers, during Operation PORTREX (Puerto Rican Training Exercise). This large scale operation simulated an attempt to recapture enemy-held Vieques Island, off the eastern end of Puerto Rico, by combined contingents of U. S. Navy, Air Force, and Army troops. A fast carrier task group, which constituted part of these forces, was composed essentially of two CV class and one CVB class carriers plus their destroyer screen. For a short time, the task group also included two CVL's and two cruisers. The following discussion is based on operations aboard the CV-47 (Philippine Sea) as observed by the members of the Avigation Branch (Radio Division III, NRL). The data is concerned solely with air operations, and in particular, with the tactics and geometry involved in short distance navigation approach and landing as they affect the problem of all-weather flying from carrier bases.

Although some of the data obtained are included in USF publications, others are not. In addition it proved to be extremely valuable for those engaged in carrier navigation research problems to witness the present methods employed in the fleet and to appreciate the operational problems encountered at sea. Only limited facilities were available for quantitative measurements of any kind, so that no claim for precision is made for the "numbers" presented here. It is hoped that, from an analysis of the present data and correlation with the laboratory work now going on, the type of additional data needed and methods for accurately obtaining it may be specified.

INTERVAL FROM CUT TO TOUCHDOWN

The CV-47 had several types of aircraft aboard for these maneuvers: F2H, F8F, AD, and TBM. The different types of aircraft aboard give an opportunity to record data on the various time factors involved in bringing the aircraft aboard. Records were taken of the time interval between the cut signal, as given by the landing signal officer, and the instant of touchdown on the deck. By noting the number of the arresting cable caught by the plane and knowing the distance from the aft end of the ship to the various cables, the distance from touchdown to the end of the deck can be calculated. Since the different approach speeds for each plane and the wind across the carrier deck are relatively constant, the aircraft speed relative to the carrier was recorded. Using the above information, an approximate figure was given for the distance between the plane and the carrier when the cut signal was given. Knowing the aircraft speed "s" as prescribed and being able to measure "d" directly, it was assumed that D + d was approximately equal to R, due to low value of the elevation angle α, hence:

$$\left(\frac{s \times 1.15 \times 6000 \times T}{3600}\right) - d = D$$

where s = Speed of plane in knots

T = Time in seconds between cut signal and touchdown

d = Approximate distance from after edge of carrier deck to the plane at touchdown

D = Distance of plane in rear of carrier when given cut signal

Table 1 summarizes the results of these computations.

TABLE 1
Distance between the Plane and Carrier at Time of "Cut"

Date	F2H	F8F	AD	TBM	All Plane Average
3-5-50	—	—	141.0	—	141.0
3-6-50	128	105.7	123.6	—	115.0
3-7-50	154	101.8	120.0	93.8	115.0

The average distance for all planes on all days was 118 feet and is based on the three day average of 100 landings.

Height Above Flight Deck

The height of aircraft above the carrier deck at the time of "cut" signal as given by the LSO, is an important bit of data in the study of carrier landing systems. The motion picture films which were taken during the trip offered a means whereby this distance could be reasonably estimated. To do this, the film frame is found on which the LSO is seen to give the actual cut signal. From this frame the following measurements are made.

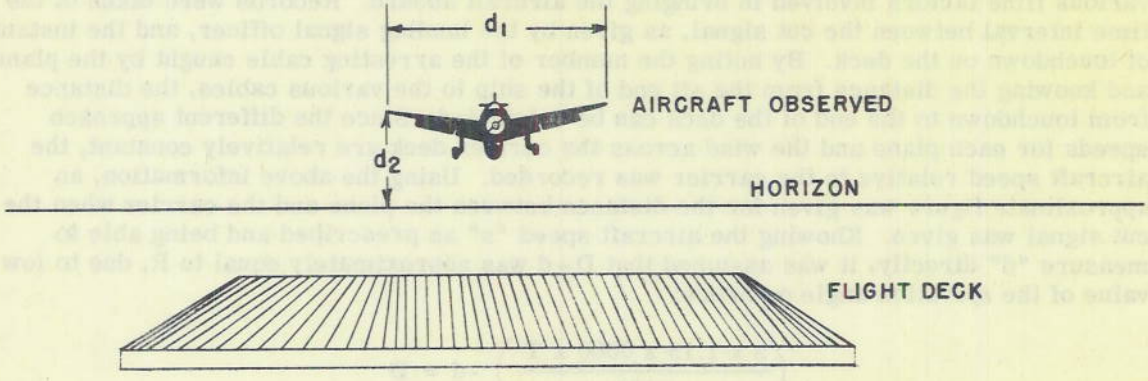

Figure A1

The measurement of d_1 and d_2 are recorded, together with the known (pre-measured) height of the camera above the flight deck. The wing span of the aircraft is known and hence a relation can be set up

$$\frac{d_2}{h_x} = \frac{d_1}{\text{wing span}} \quad \text{or} \quad \frac{\text{wing span} \times d_2}{d_1} = h_x$$

where d_1 and d_2 are measured values in same units and h_x is the distance of the aircraft above the camera position (horizon). Then the height of the aircraft above the flight deck is equal to the measured distance from the surface of the flight deck to the camera lens $\pm$ the height of the plane above or below the horizon. This, of course, assumes a perfectly level flight deck so that such data can only be valid for landings which were photographed on a calm day. In Table 2, height data results are shown.

TABLE 2
Height Above Carrier Deck at the "Cut" for Various Type Plane Landing Aboard a CV-Class Carrier

F8F	AD	F2H	TBM
29.40	41.50	27.00	29.27
31.45	33.60	19.85	31.64
37.35	32.13	19.85	
35.20	40.25		
29.70	27.27		
27.00	41.10		
32.45	43.20		
34.40			
34.40			
28.56			
29.84			
27.00			
40.00			
29.73			
33.16			
Average 31.98	37.00	22.23	30.45

DECK MOTION

The problem of motion of the Carrier deck is intimately related to the success of any carrier approach and landing system. During Operation PORTREX initial attempts were made at qualitative measurements of this motion in the pitch axis by means of a homemade accelerometer, photographic means, and stable element recording. The instrumentation was such that only the accelerometer data had the necessary resolution and readability. However, the instrument used for the acceleration data proved to be inaccurate, so that the data obtained could only be used for a qualitative analysis. These data are being reduced and at the same time a system is being assembled to record much more accurate and better correlated measurements. These results will be reported at a later date.

CARRIER LANDING PATTERN

Figure A2 shows the normal pattern flown by carrier aircraft in their approach to a landing under contact conditions. The figure is self-explanatory to a large extent. The various reasons for the choice of such a pattern include (1) visibility during the approach, (2) absorption of wave-off into the pattern, and (3) compactness in terms of linear dimensions. The recent use of jet aircraft aboard carriers practically eliminates the first reason because of the extremely good visibility from these types of aircraft.

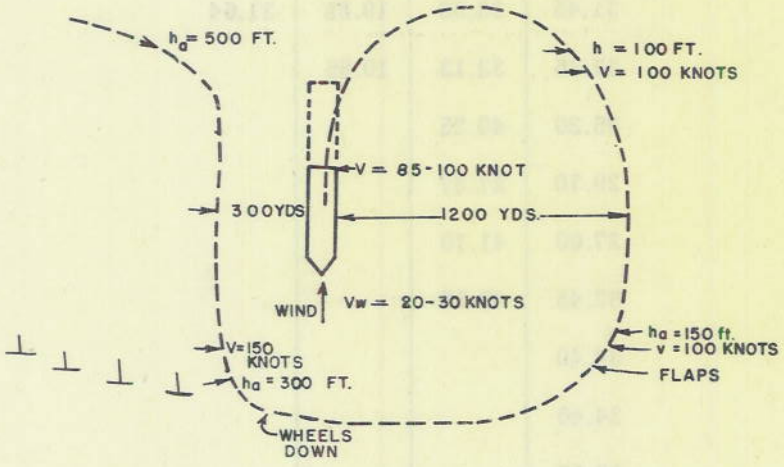

Figure A2 - Normal carrier flight pattern

RENDEZVOUS AND BREAK-UP PATTERNS

Figures A3 and A4 show respectively the rendezvous pattern for aircraft after take-off for a five carrier task force. Normally, aircraft are launched with a 20- to 30-second interval, although the use of catapults generally slows down the operations. Here again the drawings are self-explanatory.

For break-up after return from a strike, all aircraft come in on a designated YE sector over a "watch-dog" carrier for recognition. At times during the past war this recognition function was performed by one or more destroyers placed ahead of the task force.

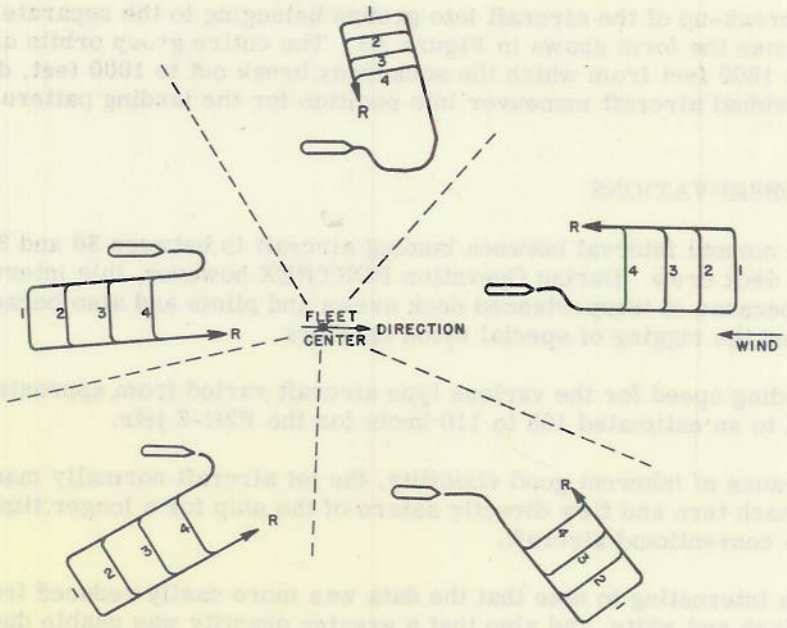

Figure A3 - Possible flight operation rendezvous after launch
(Based on carrier task force)

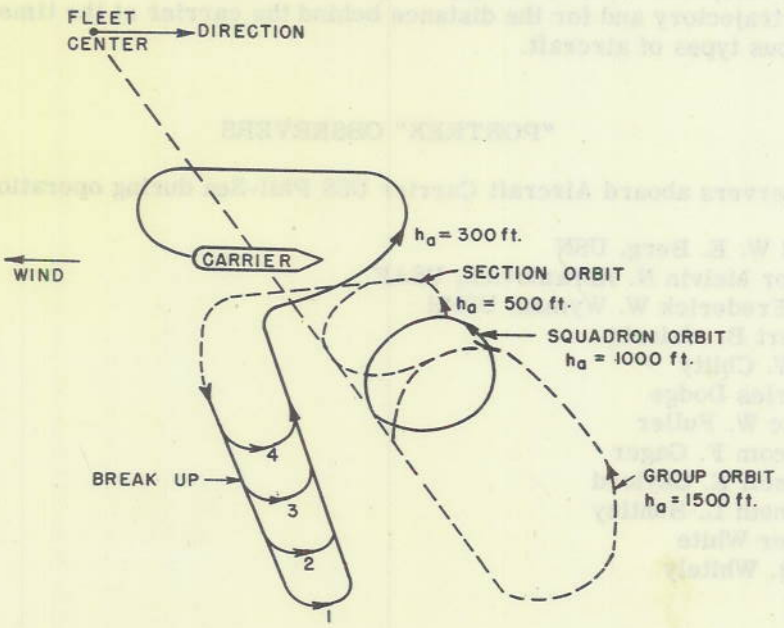

Figure A4 - Rendezvous after strike (One carrier shown)

Then, after break-up of the aircraft into groups belonging to the separate carriers, the pattern assumes the form shown in Figure A3. The entire group orbits along a designated YE sector at 1500 feet from which the squadrons break out to 1000 feet, divisions to 500 feet and individual aircraft maneuver into position for the landing pattern.

GENERAL OBSERVATIONS

(1) The normal interval between landing aircraft is between 30 and 35 seconds for a well trained deck crew. During Operation PORTREX however, this interval was close to 50 seconds because of inexperienced deck crews and pilots and also because the jet aircraft required the rigging of special nylon barriers.

(2) Landing speed for the various type aircraft varied from approximately 80 knots for the TBM to an estimated 105 to 110 knots for the F2H-2 jets.

(3) Because of inherent good visibility, the jet aircraft normally made a much wider radius approach turn and flew directly astern of the ship for a longer time and at a lower altitude than conventional aircraft.

(4) It is interesting to note that the data was more easily reduced from color film than from black and white, and also that a greater quantity was usable due to the better definition and contrast. It is therefore recommended that all such data be taken in the future on color film.

(5) It is suggested that, in order to obtain data on the trajectory of carrier landings, a movie camera be located in a helicopter directly opposite the after end on the flight deck and at a safe distance on the starboard side to photograph continually the aircraft as they land. Using a telephoto lens, seemingly very accurate data could be reduced from the film both for trajectory and for the distance behind the carrier at the time of "cut" by the LSO for various types of aircraft.

"PORTREX" OBSERVERS

NRL observers aboard Aircraft Carrier USS Phil-Sea during operation PORTREX.

CDR W. E. Berg, USN
Major Melvin N. Abramovich, USAF
LT Frederick W. Wyman, USNR
Albert Brodzinsky
H. W. Chitty
Charles Dodge
Issac W. Fuller
Malcom F. Gager
Russell E. Gaylord
Kenneth L. Huntley
Roger White
R. B. Whitely